EUROPEAN ORGANIZATION FOR NUCLEAR RESEARCH

J/ψ suppression at forward rapidity in Pb–Pb collisions at $\sqrt{s_{\mathrm{NN}}} = 5.02$ TeV

ALICE Collaboration[*]

Abstract

The inclusive J/ψ production has been studied in Pb–Pb and pp collisions at the centre-of-mass energy per nucleon pair $\sqrt{s_{\mathrm{NN}}} = 5.02$ TeV, using the ALICE detector at the CERN LHC. The J/ψ meson is reconstructed, in the centre-of-mass rapidity interval $2.5 < y < 4$ and in the transverse-momentum range $p_{\mathrm{T}} < 12$ GeV/c, via its decay to a muon pair. In this Letter, we present results on the inclusive J/ψ cross section in pp collisions at $\sqrt{s} = 5.02$ TeV and on the nuclear modification factor R_{AA}. The latter is presented as a function of the centrality of the collision and, for central collisions, as a function of the transverse momentum p_{T} of the J/ψ. The measured R_{AA} values indicate a suppression of the J/ψ in nuclear collisions and are then compared to our previous results obtained in Pb–Pb collisions at $\sqrt{s_{\mathrm{NN}}} = 2.76$ TeV. The ratio of the R_{AA} values at the two energies is also computed and compared to calculations of statistical and dynamical models. The numerical value of the ratio for central events (0–10% centrality) is $1.17 \pm 0.04(\mathrm{stat}) \pm 0.20(\mathrm{syst})$. In central events, as a function of p_{T}, a slight increase of R_{AA} with collision energy is visible in the region $2 < p_{\mathrm{T}} < 6$ GeV/c. Theoretical calculations provide a good description of the measurements, within uncertainties.

---

[*]See Appendix A for the list of collaboration members

1   Introduction

When heavy nuclei collide at ultrarelativistic energies, a state of strongly-interacting matter is formed, characterised by high temperature and density, where quarks and gluons are not confined into hadrons (Quark–Gluon Plasma, QGP [1]). A detailed characterisation of the QGP is the object, since more than 15 years, of an intense research activity at the BNL/RHIC [2–5] and CERN/LHC [6] ion colliders. Charmonia and bottomonia, which are bound states of charm-anticharm ($c\bar{c}$) or bottom-antibottom ($b\bar{b}$) quarks, respectively [7], are among the most sensitive probes of the characteristics of the QGP. A suppression of their yields in nucleus–nucleus (A–A) collisions with respect to expectations from proton–proton (pp) collisions was experimentally observed. For the J/ψ meson, the ground $c\bar{c}$ state with quantum numbers $J^{PC} = 1^{--}$, a suppression was found at both RHIC, in Au–Au interactions at the centre-of-mass energy per nucleon pair $\sqrt{s_{NN}} = 0.2$ TeV [8, 9], and at the LHC in Pb–Pb collisions at $\sqrt{s_{NN}} = 2.76$ TeV [10, 11]. Theoretical calculations predict J/ψ suppression to be induced by the screening of the colour force in a deconfined medium and to become stronger as the QGP temperature increases [12, 13]. The LHC results, integrated over transverse momentum (p_T) down to $p_T = 0$, show a suppression of the J/ψ, quantified through the ratio between its yields in Pb–Pb and those in pp, normalised to the number of nucleon–nucleon collisions in Pb–Pb (nuclear modification factor, R_{AA}). However, the observed suppression is smaller than at RHIC [14, 15], in spite of the higher initial temperature of the QGP formed at the LHC [16]. The effect is particularly evident for head-on (central) collisions. In order to explain these observations, theoretical models require a contribution from J/ψ regeneration via a recombination mechanism [17, 18] between the c and $\bar{c}$ quarks, during the deconfined phase and/or at the hadronisation of the system, which occurs when its temperature falls below the critical value $T_c \sim 155$ MeV [19]. The strength of this regeneration effect increases with the initial number of produced $c\bar{c}$ pairs relative to the total number of quarks and, therefore, increases with the collision energy, explaining the reduced suppression at the LHC. Since the bulk of charm-quark production occurs at small momenta, recombination should be more important for low-p_T J/ψ, as observed in the LHC results [15].

An important test of the suppression and regeneration picture of J/ψ production at the LHC can be obtained by comparing the centrality and p_T dependence of the J/ψ R_{AA}, measured at $\sqrt{s_{NN}} = 2.76$ TeV, to that obtained at $\sqrt{s_{NN}} = 5.02$ TeV, the highest energy available up to now in nuclear collisions. The suppression effects related to colour screening should become stronger when increasing the collision energy, due to the higher QGP temperature, and also the recombination effects should become stronger, due to the expected increase of the $c\bar{c}$ production cross section. The two effects act in opposite directions and the comparison of the R_{AA} at the different energies can provide insights in the evolution of the relative contribution of the two processes.

In this Letter, we present the first results on the J/ψ R_{AA} measured by the ALICE Collaboration in Pb–Pb collisions at $\sqrt{s_{NN}} = 5.02$ TeV and the integrated and p_T differential J/ψ production cross section in pp collisions at the same energy. In both Pb–Pb and pp collisions, the J/ψ is reconstructed via its dimuon decay channel at forward rapidity, $2.5 < y < 4$ and for $p_T < 12$ GeV/c. The measurements refer to inclusive J/ψ production, that includes both prompt J/ψ (direct J/ψ and feed-down from higher-mass resonances) and non-prompt J/ψ (from decay of beauty hadrons). The nuclear modification factor is obtained by normalising the J/ψ yield in Pb–Pb collisions to the product of the nuclear overlap function times the corresponding J/ψ cross section measured in pp, at the same energy and in the same kinematic window. The results on R_{AA} are presented as a function of the J/ψ p_T and of the centrality of the collision.

2   Experimental apparatus and data sample

The ALICE detector design and performance are extensively described in [20] and [21]. The analysis presented here is based on the detection of muons in the forward muon spectrometer [22], which covers the pseudo-rapidity range $-4 < \eta < -2.5$. In addition, the Silicon Pixel Detector (SPD) [23] is used

to reconstruct the primary vertex. The V0 detectors [24] provide a minimum-bias (MB) trigger and are used to determine the centrality of the collision, while the T0 Cherenkov counters [25] are used for the luminosity determination in pp collisions. Finally, the Zero Degree Calorimeters (ZDC) are used to reject electromagnetic Pb–Pb interactions [26]. A brief description of these detectors is given hereafter.

The muon spectrometer contains a front absorber, made of carbon, concrete and steel, placed between 0.9 and 5 m from the Interaction Point (IP), which filters out hadrons, thus decreasing the occupancy in the downstream tracking system. The latter is composed of five stations, each one consisting of two planes of Cathode Pad Chambers (CPC). The third tracking station is placed inside the gap of a dipole magnet with a 3 T·m field integral. Two trigger stations, each one equipped with two planes of Resistive Plate Chambers (RPC), are located behind a 7.2 interaction length iron wall, which absorbs secondary hadrons escaping the front absorber and low-momentum muons. The muon trigger system delivers single-muon and dimuon triggers with a programmable transverse-momentum threshold. Finally, throughout its entire length, a conical absorber around the beam pipe ($\theta < 2°$) made of tungsten, lead and steel shields the muon spectrometer against secondary particles produced by the interaction of large-η primary particles in the beam pipe.

The primary vertex is reconstructed using hit pairs in the two cylindrical layers of the SPD [20, 23], which have average radii of 3.9 and 7.6 cm, and cover the pseudo-rapidity intervals $|\eta| < 2$ and $|\eta| < 1.4$, respectively.

The two V0 detectors [24], with 32 scintillator tiles each, are placed on each side of the IP, covering the pseudo-rapidity ranges $2.8 < \eta < 5.1$ and $-3.7 < \eta < -1.7$. The coincidence of the signals from the two hodoscopes defines the MB trigger. Beam-induced background is reduced by applying timing cuts on the signals from the V0s and ZDCs. The latter are positioned along the beam direction at ±112.5 m from the IP. Finally, the T0 detectors [25], made of two arrays of quartz Cherenkov counters, are placed on both sides of the IP, covering the pseudo-rapidity intervals $-3.3 < \eta < -3$ and $4.6 < \eta < 4.9$.

In Pb–Pb collisions, the centrality determination is based on a Glauber fit of the total V0 signal amplitude distribution as described in [27, 28]. A selection corresponding to the most central 90% of the hadronic cross section was applied; for these events the MB trigger is fully efficient.

For both Pb–Pb and pp data taking, the trigger condition used in the analysis is a $\mu\mu$-MB trigger formed by the coincidence of the MB trigger and an unlike-sign (US) dimuon trigger. The latter has a trigger probability for each of the two muon candidates that increases with the muon p_{T}, is 50% at 1.0 GeV/c (0.5 GeV/c) in Pb–Pb (pp) collisions, and saturates at $p_{\mathrm{T}} \approx 2.5$ GeV/c, where it reaches a value of about 98%. Like-sign dimuon triggers were also collected, mainly for background normalisation purposes in the Pb–Pb analysis.

The data samples used in this analysis correspond to an integrated luminosity $L_{\mathrm{int}}^{\mathrm{Pb\text{-}Pb}} \approx 225\,\mu\mathrm{b}^{-1}$ for Pb–Pb and $L_{\mathrm{int}}^{\mathrm{pp}} \approx 106\,\mathrm{nb}^{-1}$ for pp collisions.

3 Data analysis

The analysis procedure was very similar for the two data samples described in this Letter. In the following paragraphs, the Pb–Pb analysis is first presented, followed by the description of the pp one.

The J/ψ candidates were formed by combining pairs of US tracks reconstructed in the geometrical acceptance of the muon spectrometer using the tracking algorithm described in [22]. The same single-muon and dimuon selection criteria as in previous analyses [15] were applied, and tracks in the tracking system were required to match a track segment in the muon trigger system (trigger tracklet).

The J/ψ raw yields were determined from the invariant mass distribution of US dimuons using two methods. In the first one, the US dimuon invariant mass distributions were fitted with the sum of a signal

and a background function. In the second approach, the background, estimated using an event-mixing technique and normalised using the like-sign dimuon distributions [15], was subtracted and the resulting spectra were fitted with the sum of a signal function and a (small) residual background component.

Various shapes were considered for the signal and background contributions. For the J/ψ signal either an extended Crystal Ball (CB2) function or a pseudo-Gaussian with a mass-dependent width were used [29]. The non-Gaussian tails of the signal functions were fixed either (i) to the values obtained in Monte Carlo (MC) simulations, where simulated J/$\psi \to \mu^+\mu^-$ are embedded into real events to account for the effect of the detector occupancy, or (ii) to the values obtained in a high-statistics pp collision sample at $\sqrt{s} = 13$ TeV, collected under similar detector conditions. The tail parameters exhibit a dependence on the p_T and rapidity of the J/ψ and a mild dependence on the centrality of the collision. The small contribution of the $\psi(2S)$ signal was taken into account in the fits, its mass and width being tied to those of the J/ψ [30]. For the background, when the US dimuon mass spectrum was fitted, a variable-width-Gaussian with a mass-dependent width or the ratio of a 2nd to a 3rd order polynomial were used. When considering the US dimuon distributions after subtraction of the background obtained with the event-mixing procedure, a small dimuon continuum component is still present and was fitted using the sum of two exponentials. Several fitting sub-ranges, within the interval $2 < m_{\mu\mu} < 5$ GeV/c^2, were used for both signal extraction procedures.
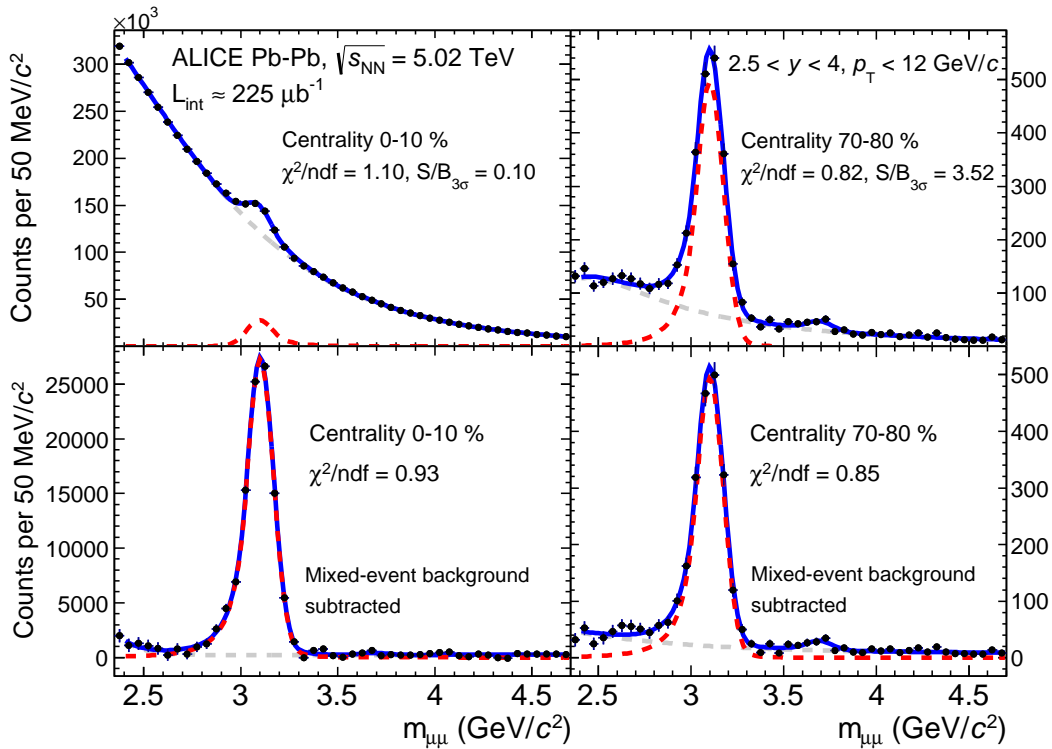

Fig. 1: (colour online). Invariant mass distributions of US dimuons with $2.5 < y < 4$ and $p_T < 12$ GeV/c. The top (bottom) row shows the distribution before (after) background subtraction with the event-mixing technique. The left panels correspond to the most central events (0–10%) while the right panels to a peripheral (70–80%) centrality range. The fit curves shown in blue represent the sum of the signal and background shapes, while the red lines correspond to the J/ψ signal and the grey ones to the background.

Figure 1 shows examples of fits to the US dimuon invariant mass distributions with and without background subtraction using the event-mixing technique, for different selections in centrality. The raw J/ψ yield in each centrality or p_T interval was determined as the average of the results obtained with

the two fitting approaches, the various parametrisations of signal and background and the different fitting ranges, while the corresponding systematic uncertainties were defined as the RMS of these results. A further contribution to the systematic uncertainty was estimated by using a different set of resonance tails obtained using in the MC simulation a different particle transport model (GEANT4 [31] instead of GEANT3 [32]). The total number of J/ψ, integrated over centrality, p_T and y, is $N_{J/\psi} = 2.77 \pm 0.02(\text{syst}) \pm 0.05(\text{syst}) \cdot 10^5$. The systematic uncertainty ranges from 1.6% to 2.8% as a function of centrality and from 1.2% to 3.1% as a function of p_T.

The nuclear modification factor, as a function of the centrality class i of the collision and for the J/ψ transverse-momentum interval Δp_T, is calculated as

$$R_{AA}^i(\Delta p_T) = \frac{N_{J/\psi}^i(\Delta p_T)}{BR_{J/\psi \to \mu^+\mu^-} N_{MB}^i A\varepsilon^i(\Delta p_T)\langle T_{AA}^i \rangle \sigma_{J/\psi}^{pp}(\Delta p_T)}, \tag{1}$$

where $N_{J/\psi}^i(\Delta p_T)$ is the number of extracted J/ψ in a given centrality and p_T range, $BR_{J/\psi \to \mu^+\mu^-} = 5.96 \pm 0.03\%$ is the branching ratio of the dimuon decay channel [33], N_{MB}^i is the number of equivalent minimum-bias events, $A\varepsilon^i(\Delta p_T)$ is the product of the detector acceptance times the reconstruction efficiency, $\langle T_{AA}^i \rangle$ is the average of the nuclear overlap function, and $\sigma_{J/\psi}^{pp}(\Delta p_T)$ is the inclusive J/ψ cross section for pp collisions at the same energy and in the same kinematic range as the Pb–Pb data.

The $A\varepsilon$ values were determined from MC simulations, with the generated p_T and y distributions for the J/ψ adjusted on data, and separately tuned for each centrality class using an iterative approach. Unpolarised J/ψ production was assumed [15]. For the tracking chambers, the time-dependent status of each electronic channel during the data taking period was taken into account as well as the misalignment of the detection elements. The efficiencies of the muon trigger chambers were determined from data and were then applied in the simulations. Finally, the dependence of the efficiency on the detector occupancy was taken into account by embedding MC-generated J/ψ into real minimum-bias Pb–Pb events.

For J/ψ produced within $2.5 < y < 4$ and $p_T < 12$ GeV/c, in 0–90% most central collisions, the $A\varepsilon$ value is $0.136 \pm 0.007(\text{syst})$. A relative decrease of the efficiency by 14% was observed when going from peripheral to central collisions. As a function of p_T, $A\varepsilon$ has a minimum value of about 0.12 at $p_T \approx 1.5$ GeV/c, and then steadily increases up to about 0.4 at the upper end of the considered range. The following sources of systematic uncertainty on $A\varepsilon$ were considered. A first contribution of 2% due to the input MC p_T and y distributions was estimated by (i) varying the input shapes that were tuned on data within their statistical uncertainties and (ii) taking into account the effect of possible $p_T - y$ correlations by comparing, as a function of centrality, the $A\varepsilon$ values with the corresponding result of a 2-D acceptance calculation in classes of p_T and y. A second contribution comes from the tracking efficiency and it was estimated by comparing the single-muon tracking efficiency values obtained, in MC and data, with a procedure that exploits the redundancy of the tracking-chamber information [15]. A 3% systematic uncertainty on the dimuon tracking efficiency is obtained and is approximately constant as a function of centrality and kinematics. The systematic uncertainty on the dimuon trigger efficiency represents the third contribution and it has two origins: the intrinsic efficiencies of the muon trigger chambers and the response of the trigger algorithm. The first one was determined from the uncertainties on the trigger chamber efficiencies measured from data and applied to simulations and it amounts to 1.5%. The second one was estimated by comparing the p_T dependence, at the single-muon level, of the trigger response function between data and MC and it varies between 0.2% and 4.6% as a function of p_T. Combining the two sources, a systematic uncertainty ranging from 1.5% to 4.8% as a function of the J/ψ p_T is obtained. Finally, there is a 1% contribution related to the choice of the χ^2 cut used in defining the matching between the reconstructed tracks and the trigger tracklets.

The normalisation factor to the number of equivalent MB events was obtained as $N_{MB}^i = F^i \cdot N_{\mu\mu\text{-MB}}$, where $N_{\mu\mu\text{-MB}}$ is the number of $\mu\mu$-MB triggered events, and F^i is the inverse of the probability of

having a dimuon trigger in a MB event in the centrality range i. The F^i values were calculated with two different methods, by applying the dimuon trigger condition in the analysis on minimum-bias events, or from the relative counting rate of the two triggers [34]. The obtained value, in the 0–90% centrality class, is $F = 11.84 \pm 0.06$, where the uncertainty is dominated by a systematic contribution corresponding to the difference between the results obtained with the two approaches. As a function of centrality, $F^i = F \cdot \Delta^i$, where Δ^i is the fraction of the inelastic cross section of a given centrality class with respect to the whole 0–90% centrality range (e.g. 0.1/0.9 for 0–10% centrality and so on).

The values for $\langle T_{\mathrm{AA}}^i \rangle$ and for the average number of participant nucleons $\langle N_{\mathrm{part}}^i \rangle$ were obtained via a Glauber calculation [27, 35]. The systematic uncertainty is 3.2% for the 0–90% centrality range and was obtained by varying within uncertainties the density parameters of the Pb nucleus and the nucleon–nucleon inelastic cross section [36].

Finally, the effects of the uncertainty on the value of the V0 signal amplitude corresponding to 90% of the hadronic Pb–Pb cross section were estimated by varying such a value by $\pm 0.5\%$ [27] and redefining correspondingly the centrality intervals. The systematic effect on R_{AA} ranges from 0.1% to 6.6% from central to peripheral collisions.

The J/ψ cross-section values in pp collisions at $\sqrt{s} = 5.02$ TeV, both integrated and p_{T} differential, were obtained with an analysis procedure similar to the one described in the previous paragraphs for Pb–Pb. In particular, the same criteria for single-muon and dimuon selection were adopted.

The signal extraction was then performed by fitting the spectra with the sum of a signal and a background contribution, using shapes similar to those adopted for the Pb–Pb analysis. The background subtraction via the event-mixing technique was not used, as the signal-over-background ratio is larger by a factor ~ 40, in the p_{T}-integrated spectra, with respect to central Pb–Pb collisions, making the influence of the background estimate much less important in the determination of the uncertainty on $N_{\mathrm{J}/\psi}^{\mathrm{pp}}$. The value $N_{\mathrm{J}/\psi}^{\mathrm{pp}} = 8649 \pm 123(\mathrm{stat}) \pm 297(\mathrm{syst})$ is obtained, with the systematic uncertainty determined as for the Pb–Pb analysis.

The determination of $A\varepsilon_{\mathrm{pp}}$ was carried out via MC simulations. Since no appreciable dependence of the tracking efficiency as a function of the hadronic multiplicity can be seen in pp, a pure MC (i.e., without embedding) was used. The input p_{T} and y distributions were obtained from the measured ones via an iterative procedure, and unpolarised J/ψ production was assumed [37]. The obtained value is $A\varepsilon_{\mathrm{pp}} = 0.243 \pm 0.007(\mathrm{syst})$, with the systematic uncertainties on the tracking, trigger and matching efficiency calculated as in the Pb–Pb analysis. Because of the limited pp statistics, the systematic uncertainty on the MC inputs was not obtained through a 2-D acceptance calculation, as done in the Pb–Pb analysis, but it was determined comparing the $A\varepsilon$ values obtained using J/ψ p_{T} (y) distributions evaluated in various y (p_{T}) intervals in pp collisions at $\sqrt{s} = 7$ TeV [38].

The integrated luminosity was calculated as $L_{\mathrm{int}}^{\mathrm{pp}} = (N_{\mu\mu\text{-MB}}^{\mathrm{pp}} \cdot F^{\mathrm{pp}})/\sigma_{\mathrm{ref}}^{\mathrm{pp}}$, where $\sigma_{\mathrm{ref}}^{\mathrm{pp}}$ is a reference-trigger cross section measured in a van der Meer scan, following the procedure detailed in [39], and F^{pp} is the ratio of the reference-trigger probability to the $\mu\mu$-MB trigger probability. The corresponding numerical value is $L_{\mathrm{int}}^{\mathrm{pp}} = 106.3 \pm 2.2(\mathrm{syst})$ nb^{-1}, where the quoted uncertainty reflects the van der Meer scan uncertainty.

Finally, the inclusive J/ψ cross section in pp collisions at $\sqrt{s} = 5.02$ TeV was obtained as

$$\frac{\mathrm{d}^2 \sigma_{\mathrm{J}/\psi}^{\mathrm{pp}}}{\mathrm{d}y \mathrm{d}p_{\mathrm{T}}} = \frac{N_{\mathrm{J}/\psi}^{\mathrm{pp}}(\Delta p_{\mathrm{T}})}{\mathrm{BR}_{\mathrm{J}/\psi \to \mu^+\mu^-} L_{\mathrm{int}}^{\mathrm{pp}} A\varepsilon_{\mathrm{pp}}(\Delta p_{\mathrm{T}}) \Delta p_{\mathrm{T}} \Delta y}. \tag{2}$$

Table 1 summarises the systematic uncertainties on the measurement of the nuclear modification factors and $\mathrm{d}^2 \sigma_{\mathrm{J}/\psi}^{\mathrm{pp}}/\mathrm{d}y \mathrm{d}p_{\mathrm{T}}$.

Source	R_{AA}			$\mathrm{d}^2\sigma^{\mathrm{pp}}_{\mathrm{J}/\psi}/\mathrm{d}y\mathrm{d}p_{\mathrm{T}}$	
	0–90% $p_{\mathrm{T}} < 12$ GeV/c	vs p_{T} (0–20%)	vs centrality ($p_{\mathrm{T}} < 8$ GeV/c)	$p_{\mathrm{T}} < 12$ GeV/c	vs p_{T}
Signal extr.	1.8	1.2–3.1	1.6–2.8	3	1.5–9.3
MC input	2	2	2*	2	0.7–1.5
Tracking eff.	3	3	3*	1	1
Trigger eff.	3.6	1.5–4.8	3.6*	1.8	1.5–1.8
Matching eff.	1	1	1*	1	1
F ($L^{\mathrm{pp}}_{\mathrm{int}}$)	0.5	0.5*	0.5*	(2.1)	(2.1*)
BR	-	-	-	0.5	0.5*
$\langle T_{\mathrm{AA}} \rangle$	3.2	3.2*	3.1–7.6		
Centrality	0	0.1*	0–6.6		
pp reference	5.0	3–10 $\oplus$ 2.1*($L^{\mathrm{pp}}_{\mathrm{int}}$)	4.9*		

Table 1: Summary of systematic uncertainties, in percentage, on R_{AA} and $\mathrm{d}^2\sigma^{\mathrm{pp}}_{\mathrm{J}/\psi}/\mathrm{d}y\mathrm{d}p_{\mathrm{T}}$. Values marked with an asterisk correspond to correlated uncertainties as a function of p_{T} (second and fifth column) or centrality (third column). There is no correlation between the uncertainties related to the analysis of the Pb–Pb and of the pp sample. The contents of the "pp reference" row correspond to the quadratic sum of the contributions indicated for $\mathrm{d}^2\sigma^{\mathrm{pp}}_{\mathrm{J}/\psi}/\mathrm{d}y\mathrm{d}p_{\mathrm{T}}$, excluding only the BR uncertainty which cancels out when forming the R_{AA}.

The R_{AA} values presented in the following refer to inclusive J/ψ production, i.e. include both prompt and non-prompt J/ψ. Since beauty-hadron decays occur outside the QGP, the non-prompt J/ψ R_{AA} is related to the nuclear modification of the beauty-hadron p_{T} distributions. The difference between the R_{AA} of prompt and inclusive J/ψ can be estimated as in [15], using the fraction F_{B} of non-prompt to inclusive J/ψ in pp collisions and assuming two extreme cases for the $R^{\mathrm{non\text{-}prompt}}_{\mathrm{AA}}$ of non-prompt J/ψ, namely no medium effects on b-quarks or their complete suppression. F_{B} was obtained by an interpolation of the LHCb measurements in pp collisions at $\sqrt{s} = 2.76$ and 7 TeV [38, 40, 41]. The quantitative effect on the inclusive J/ψ R_{AA} is provided in the following along with the results.

4 Results

The p_{T}-differential inclusive J/ψ cross section in pp collisions at $\sqrt{s} = 5.02$ TeV, in the region $2.5 < y < 4$, is shown in Fig. 2. The cross section value, integrated over the interval $2.5 < y < 4$, $p_{\mathrm{T}} < 12$ GeV/c is $\sigma^{\mathrm{pp}}_{\mathrm{J}/\psi} = 5.61 \pm 0.08(\mathrm{stat}) \pm 0.28(\mathrm{syst})$ μb. These results are used as a reference in the determination of the nuclear modification factor for Pb–Pb collisions. Both the differential and integrated pp cross section values are consistent with those obtained via an interpolation [40, 42] of the measured values at $\sqrt{s} = 2.76$ and 7 TeV [43, 44], which were used for the determination of the nuclear modification factor in p–Pb collisions at $\sqrt{s_{\mathrm{NN}}} = 5.02$ TeV [34, 42, 45].

The nuclear modification factor for inclusive J/ψ production in Pb–Pb collisions at $\sqrt{s_{\mathrm{NN}}} = 5.02$ TeV, integrated over the centrality range 0–90%, and for the interval $2.5 < y < 4$, $p_{\mathrm{T}} < 12$ GeV/c is $R_{\mathrm{AA}}(p_{\mathrm{T}} < 12 \text{ GeV}/c) = 0.65 \pm 0.01(\mathrm{stat}) \pm 0.05(\mathrm{syst})$, showing a significant suppression of the J/ψ with respect to pp collisions at the same energy. When restricting the p_{T} range to 8 GeV/c, corresponding to the interval covered in the $\sqrt{s_{\mathrm{NN}}} = 2.76$ TeV results, one obtains $R_{\mathrm{AA}}(p_{\mathrm{T}} < 8 \text{ GeV}/c) = 0.66 \pm 0.01(\mathrm{stat}) \pm 0.05(\mathrm{syst})$. The ratio between the latter value and the corresponding one at $\sqrt{s_{\mathrm{NN}}} = 2.76$ TeV, $R_{\mathrm{AA}}(p_{\mathrm{T}} < 8 \text{ GeV}/c) = 0.58 \pm 0.01(\mathrm{stat}) \pm 0.09(\mathrm{syst})$ [14], is $1.13 \pm 0.02(\mathrm{stat}) \pm 0.18(\mathrm{syst})$. When calculating the ratio, the quoted uncertainties on the two values are considered as uncorrelated, except for the $\langle T_{\mathrm{AA}} \rangle$ contribution.

Figure 3 shows the centrality dependence of R_{AA} at $\sqrt{s_{\mathrm{NN}}} = 5.02$ TeV. The results are compared to the values obtained at $\sqrt{s_{\mathrm{NN}}} = 2.76$ TeV [14], and correspond to the same transverse-momentum range,
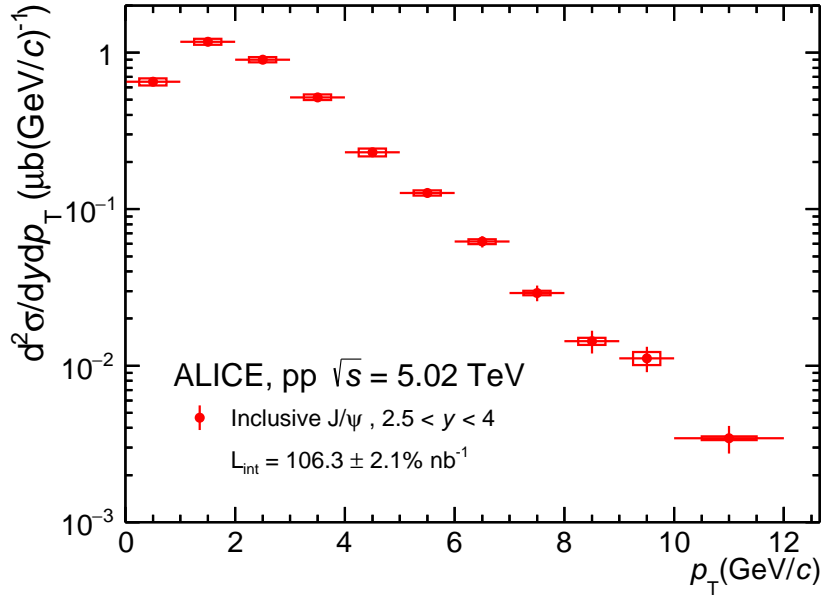
Fig. 2: (colour online). The differential cross section $d^2\sigma_{J/\psi}^{pp}/dydp_T$ for inclusive J/ψ production in pp collisions at $\sqrt{s} = 5.02$ TeV. The error bars represent the statistical uncertainties, the boxes around the points the uncorrelated systematic uncertainties. The uncertainty on the luminosity measurement represents a correlated global uncertainty.
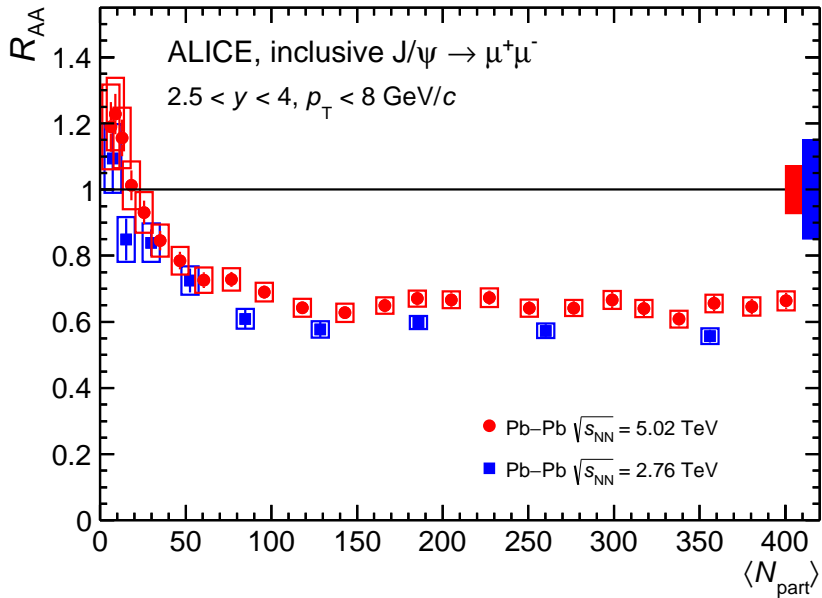

Fig. 3: (colour online). The nuclear modification factor for inclusive J/ψ production, as a function of centrality, at $\sqrt{s_{NN}} = 5.02$ TeV, compared to published results at $\sqrt{s_{NN}} = 2.76$ TeV [14]. The error bars represent statistical uncertainties, the boxes around the points uncorrelated systematic uncertainties, while correlated global uncertainties are shown as a filled box around $R_{AA} = 1$. The widths of the centrality classes used in the J/ψ analysis at $\sqrt{s_{NN}} = 5.02$ TeV are 2% from 0 to 12%, then 3% up to 30% and 5% for more peripheral collisions.

$p_T < 8$ GeV/c. The centrality dependence, characterised by an increasing suppression with centrality up to $N_{part} \sim 100$, followed by an approximately constant R_{AA} value, is similar at the two energies. A systematic difference by about 15% is visible when comparing the two sets of results, even if the effect is within the total uncertainty of the measurements. The R_{AA} of prompt J/ψ would be about 10% higher if $R_{AA}^{non-prompt} = 0$ and about 5% (1%) smaller if $R_{AA}^{non-prompt} = 1$ for central (peripheral) collisions.

An excess of very-low p_T J/ψ, compared to the yield expected assuming a smooth evolution of the J/ψ hadro-production and nuclear modification factor was observed in peripheral Pb–Pb collisions at $\sqrt{s_{NN}} = 2.76$ TeV [46]. This excess might originate from the photo-production of J/ψ and could influence the R_{AA} in peripheral collisions. To quantify the expected difference between the hadronic J/ψ R_{AA} and the measured values the method described in [15] was adopted. The hadronic J/ψ R_{AA}, for $0 < p_T < 8$ GeV/c, is estimated to be about 34%, 17% and 9% smaller than the measured values in the 80–90%, 70–80% and 60–70% centrality classes, respectively. The variation decreases to about 9%, 4% and 2%, respectively, when considering the R_{AA} for J/ψ with $0.3 < p_T < 8$ GeV/c, due to the remaining small contribution of photo-produced J/ψ. Figure 4 shows R_{AA} as a function of centrality, for $0.3 < p_T < 8$ GeV/c.
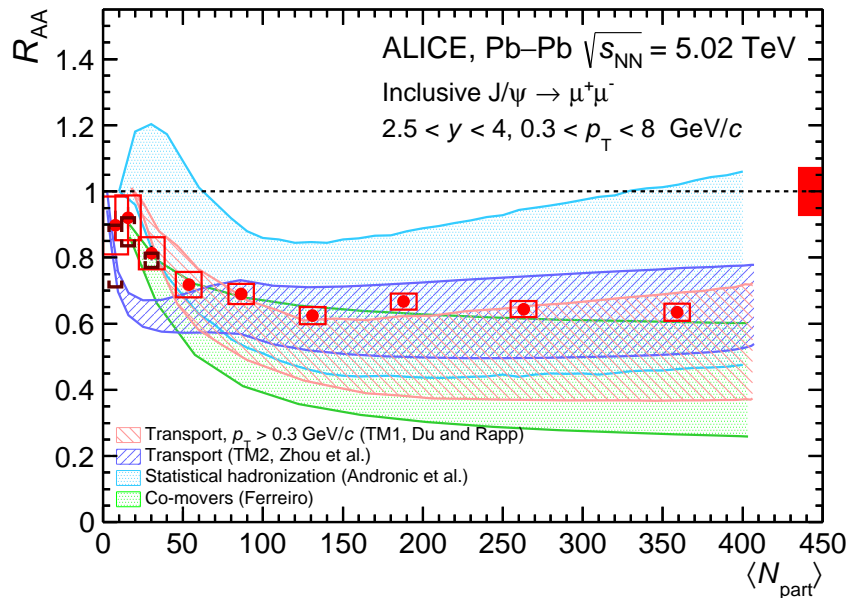

Fig. 4: (colour online). Comparison of the centrality dependence (with 10% width centrality classes) of the inclusive J/ψ R_{AA} for $0.3 < p_T < 8$ GeV/c with theoretical models [47–52]. The model predictions do not include the p_T cut, which was anyway found to have a negligible impact, since they only include hadronic J/ψ production. The error bars represent the statistical uncertainties, the boxes around the data points the uncorrelated systematic uncertainties, while the correlated global uncertainty is shown as a filled box around $R_{AA} = 1$. The brackets shown in the three most peripheral centrality intervals represent the range of variation of the hadronic J/ψ R_{AA} under extreme hypothesis on the photo-production contamination on the inclusive R_{AA}.

Comparing the results of Fig. 3 and Fig. 4, a less pronounced increase of R_{AA} for peripheral events can indeed be seen when such a selection is introduced. The same extreme hypotheses as in [15] were made to define upper and lower limits, represented with brackets on Fig. 4. Thus, the selection of J/ψ with $p_T > 0.3$ GeV/c makes the results more suitable for a comparison with theoretical models that only include hadronic J/ψ production.

We start by comparing the results to a calculation based on a statistical model approach [47], where J/ψ are created, like all other hadrons, only at chemical freeze-out according to their statistical weights.

In this model, the nucleon–nucleon $c\bar{c}$ cross section is extrapolated from LHCb pp measurements at $\sqrt{s} = 7$ TeV [53] using FONLL calculations [54], obtaining $\mathrm{d}\sigma_{c\bar{c}}/\mathrm{d}y = 0.32$ mb in the y range covered by the data. The nuclear modification of the parton distribution functions (shadowing) is accounted for via the EPS09 NLO parameterisation [55]. A 20% uncertainty on $\mathrm{d}\sigma_{c\bar{c}}/\mathrm{d}y$ is assumed when calculating the uncertainty bands for this model. The results are also compared to the calculations of a transport model (TM1) [50, 51] based on a thermal rate equation, which includes continuous dissociation and regeneration of the J/ψ both in the QGP and in the hadronic phase. The inclusive $c\bar{c}$ cross section is taken as $\mathrm{d}\sigma_{c\bar{c}}/\mathrm{d}y = 0.57$ mb, consistent with FONLL calculations, while the J/ψ production cross section value in N–N collisions is $\mathrm{d}\sigma_{\mathrm{J}/\psi}/\mathrm{d}y = 3.14$ μb. The results of this model are shown as a band where the upper limit corresponds to the case of no shadowing effects and the lower limit to a shadowing obtained from the EPS09 NLO parameterisation for central Pb–Pb collisions. The results are then compared to the predictions of a second transport model (TM2) [52], which implements a hydrodynamic description of the medium evolution. The input nucleon–nucleon cross sections for $c\bar{c}$ and J/ψ are taken as $\mathrm{d}\sigma_{c\bar{c}}/\mathrm{d}y = 0.82$ mb, corresponding to the upper limit of FONLL calculations, and $\mathrm{d}\sigma_{\mathrm{J}/\psi}/\mathrm{d}y = 3.5$ μb. Also for this model the band corresponds to the choice of either no shadowing, or a shadowing effect estimated with the EPS09 NLO parameterisation. Finally, the data are compared to a 'co-mover' model [48, 49], where the J/ψ are dissociated via interactions with the partons/hadrons produced in the same rapidity range, using an effective interaction cross section $\sigma^{\mathrm{co\text{-}J}/\psi} = 0.65$ mb, based on calculations that described lower energy experimental results. Regeneration effects are included, based on $\mathrm{d}\sigma_{c\bar{c}}/\mathrm{d}y$ values ranging from 0.45 to 0.7 mb, which correspond to the uncertainty band shown for the model. Shadowing effects, calculated within the Glauber-Gribov theory [56], are included and are consistent with EKS98/nDSg predictions [57, 58]. Finally, the contribution of non-prompt production is taken into account in the transport models TM1 and TM2, while it is not considered in the other calculations.

The data are described by the various calculations, the latter having rather large uncertainties, due to the choice of the corresponding input parameters, and in particular of $\mathrm{d}\sigma_{c\bar{c}}/\mathrm{d}y$. It can be noted that for most calculations a better description is found when considering their upper limit. For transport models this corresponds to the absence of nuclear shadowing, which can be clearly considered as an extreme assumption for primary J/ψ, considering the J/ψ measurements in p–Pb collisions [42, 45].

A correlation between the parameters of the models is present when comparing their predictions for $\sqrt{s_{\mathrm{NN}}} = 2.76$ and 5.02 TeV. Therefore, the theoretical uncertainties can be reduced by forming the ratio $r = R_{\mathrm{AA}}(5.02\ \mathrm{TeV})/R_{\mathrm{AA}}(2.76\ \mathrm{TeV})$. Concerning data, the uncertainties on $\langle T_{\mathrm{AA}} \rangle$ cancel. In Fig. 5 the centrality dependence of r, calculated for $0.3 < p_{\mathrm{T}} < 8$ GeV/c, is shown and compared to models. For prompt J/ψ the ratio r would be about 2% (1–2%) higher if beauty hadrons were fully (not) suppressed by the medium. The transport model of Ref. [50, 51] (TM1) predicts a decrease of r with increasing centrality, due to the larger suppression effects at high energy, followed by an increase, related to the effect of regeneration, which acts in the opposite direction and becomes dominant for central collisions. The other transport model (TM2) [52] also exhibits an increase for central collisions, while for peripheral collisions the behaviour is different. In the co-mover model [48, 49], no structure is visible as a function of centrality, and the calculation favours r-values slightly below unity, implying that in this model the increase of the suppression effects with energy may be dominant over the regeneration effects for all centralities. Finally, the statistical model [47] shows a continuous increase of r with centrality, dominated by the increase in the $c\bar{c}$ cross section with energy. The uncertainty bands shown in Fig. 5 correspond to variations of about 5% in the $c\bar{c}$ cross section at $\sqrt{s_{\mathrm{NN}}} = 5.02$ TeV. The data are, within uncertainties, compatible with the theoretical models, and show no clear centrality dependence. The ratio for central collisions and $0.3 < p_{\mathrm{T}} < 8$ GeV/c is $r^{0-10\%} = 1.17 \pm 0.04(\mathrm{stat}) \pm 0.20(\mathrm{syst})$.

Finally, the study of the p_{T} dependence of R_{AA} has proven to be a sensitive test of the presence of a regeneration component which, in calculations, leads to an increase at low p_{T}. Figure 6 shows, for the centrality interval 0–20%, R_{AA} as a function of transverse momentum, compared to the corresponding
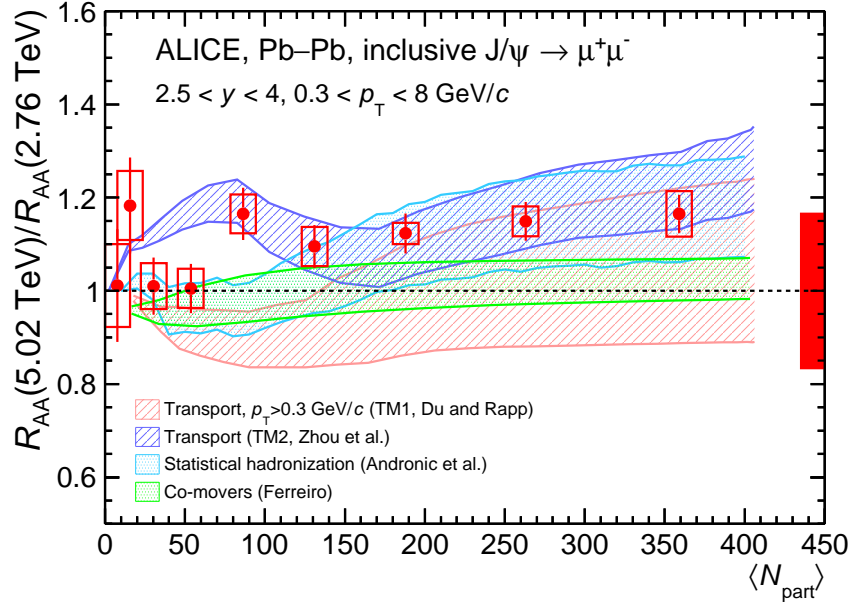
Fig. 5: (colour online). The ratio of the inclusive J/ψ R_{AA} for $0.3 < p_T < 8$ GeV/c between $\sqrt{s_{NN}} = 5.02$ and 2.76 TeV, compared to theoretical models [47–52], shown as a function of centrality. The model predictions do not include the p_T cut, which was anyway found to have a negligible impact, since they only include hadronic J/ψ production. The error bars represent the statistical uncertainties, the boxes around the data points the uncorrelated systematic uncertainties, while the correlated global uncertainty is shown as a filled box around $r = 1$.

results obtained at $\sqrt{s_{NN}} = 2.76$ TeV, and to theoretical models. The region $p_T < 0.3$ GeV/c was not excluded, because the contribution of J/ψ photo-production is negligible with respect to the hadronic one for central events [46]. In the same figure the p_T dependence of r is also shown. A hint for an increase of R_{AA} with $\sqrt{s_{NN}}$ is visible in the region $2 < p_T < 6$ GeV/c, while the results are consistent elsewhere. The prompt J/ψ R_{AA} is expected to be 7% larger (2% smaller) for $p_T < 1$ GeV/c and 30% larger (55% smaller) for $10 < p_T < 12$ GeV/c when the beauty contribution is fully (not) suppressed. Assuming that $R_{AA}^{\text{non-prompt}}$ does not vary significantly between the two collision energies, the ratio r appears to be less sensitive to the non-prompt J/ψ contribution. The effect is negligible for the case of full suppression of beauty hadrons, while it varies from no increase at low transverse momentum up to a maximum increase of about 15% for $5 < p_T < 6$ GeV/c if no suppression is assumed. The transport model of Ref. [50, 51] (TM1) describes the data at low p_T, but the overall shape of the p_T dependence is steeper in the model, which tends to underestimate the data at intermediate p_T ($3 < p_T < 7$ GeV/c).

5 Conclusion

We reported the ALICE measurement of inclusive J/ψ production in pp and Pb–Pb collisions at $\sqrt{s_{NN}} = 5.02$ TeV at the LHC. A systematic difference by about 15% is visible when comparing the R_{AA} measured at $\sqrt{s_{NN}} = 5.02$ TeV to the one obtained at $\sqrt{s_{NN}} = 2.76$ TeV, even if such an effect is within the total uncertainty of the measurements. When removing very-low p_T J/ψ ($p_T < 0.3$ GeV/c), the R_{AA} shows a less pronounced increase for peripheral events, which can be ascribed to the removal of a large fraction of electromagnetic J/ψ production [46]. These results, as well as those on the ratio of the nuclear modification factors between $\sqrt{s_{NN}} = 5.02$ and 2.76 TeV, are described by theoretical calculations, and closer to their upper limits. The p_T dependence of R_{AA} exhibits an increase at low p_T, a feature that in the model which is compared to the data is related to an important contribution of regenerated J/ψ. A hint for an increase of R_{AA} between $\sqrt{s_{NN}} = 2.76$ and 5.02 TeV is visible in the region $2 < p_T < 6$ GeV/c, while the results are consistent elsewhere. The results presented in this paper confirm that also at the highest
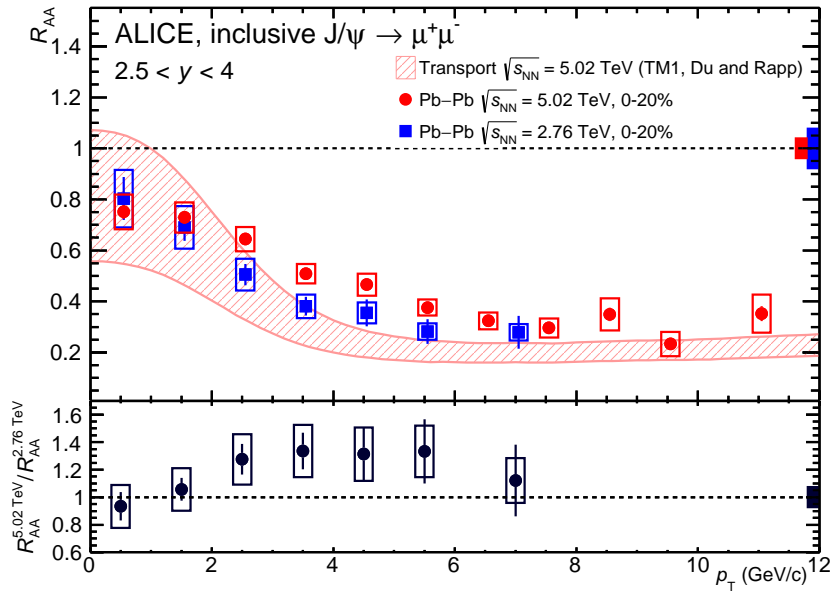
Fig. 6: (colour online). The p_T dependence of the inclusive J/ψ R_{AA} at $\sqrt{s_{NN}} = 5.02$ TeV, compared to the corresponding result at $\sqrt{s_{NN}} = 2.76$ TeV [14] and to the prediction of a transport model [50, 51](TM1), in the centrality interval 0–20%. The p_T dependence of r is also shown. The error bars represent statistical uncertainties, the boxes around the points uncorrelated systematic uncertainties, while correlated global uncertainties are shown as a filled box around $R_{AA} = 1$.

energies reached today at the LHC, data on J/ψ production support a picture where a combination of suppression and regeneration takes place in the QGP, the two mechanisms being dominant at high and low p_T, respectively.

Acknowledgements

References

[1] E. V. Shuryak, "Quark-Gluon Plasma and Hadronic Production of Leptons, Photons and Psions," *Phys. Lett.* **B78** (1978) 150. [Yad. Fiz.28,796(1978)].

[2] **BRAHMS** Collaboration, I. Arsene *et al.*, "Quark gluon plasma and color glass condensate at RHIC? The Perspective from the BRAHMS experiment," *Nucl. Phys.* **A757** (2005) 1–27, `arXiv:nucl-ex/0410020 [nucl-ex]`.

[3] **PHOBOS** Collaboration, B. B. Back *et al.*, "The PHOBOS perspective on discoveries at RHIC," *Nucl. Phys.* **A757** (2005) 28–101, `arXiv:nucl-ex/0410022 [nucl-ex]`.

[4] **STAR** Collaboration, J. Adams *et al.*, "Experimental and theoretical challenges in the search for the quark gluon plasma: The STAR Collaboration's critical assessment of the evidence from RHIC collisions," *Nucl. Phys.* **A757** (2005) 102–183, `arXiv:nucl-ex/0501009 [nucl-ex]`.

[5] **PHENIX** Collaboration, K. Adcox *et al.*, "Formation of dense partonic matter in relativistic nucleus-nucleus collisions at RHIC: Experimental evaluation by the PHENIX collaboration," *Nucl. Phys.* **A757** (2005) 184–283, `arXiv:nucl-ex/0410003 [nucl-ex]`.

[6] B. Müller, J. Schukraft, and B. Wyslouch, "First Results from Pb+Pb collisions at the LHC," *Ann. Rev. Nucl. Part. Sci.* **62** (2012) 361–386, `arXiv:1202.3233 [hep-ex]`.

[7] N. Brambilla, S. Eidelman, B. Heltsley, R. Vogt, G. Bodwin, *et al.*, "Heavy quarkonium: progress, puzzles, and opportunities," *Eur. Phys. J.* **C71** (2011) 1534, `arXiv:1010.5827 [hep-ph]`.

[8] **PHENIX** Collaboration, A. Adare *et al.*, "J/ψ suppression at forward rapidity in Au+Au collisions at $\sqrt{s_{NN}} = 200$ GeV," *Phys. Rev.* **C84** (2011) 054912, `arXiv:1103.6269 [nucl-ex]`.

[9] **STAR** Collaboration, B. I. Abelev *et al.*, "J/ψ production at high transverse momentum in p+p and Cu+Cu collisions at $\sqrt{s_{\mathrm{NN}}} = 200$ GeV," *Phys. Rev.* **C80** (2009) 041902, `arXiv:0904.0439 [nucl-ex]`.

[10] **ALICE** Collaboration, B. Abelev *et al.*, "J/ψ Suppression at Forward Rapidity in Pb-Pb Collisions at $\sqrt{s_{\mathrm{NN}}} = 2.76$ TeV," *Phys. Rev. Lett.* **109** no. 7, (Aug., 2012) 072301, `arXiv:1202.1383 [hep-exp]`.

[11] **CMS** Collaboration, S. Chatrchyan *et al.*, "Suppression of non-prompt J/ψ, prompt J/ψ, and Y(1S) in PbPb collisions at $\sqrt{s_{\mathrm{NN}}} = 2.76$ TeV," *JHEP* **05** (2012) 063, `arXiv:1201.5069 [nucl-ex]`.

[12] T. Matsui and H. Satz, "J/ψ Suppression by Quark-Gluon Plasma Formation," *Phys. Lett.* **B178** (1986) 416.

[13] S. Digal, P. Petreczky, and H. Satz, "Quarkonium feed down and sequential suppression," *Phys. Rev.* **D64** (2001) 094015, `arXiv:hep-ph/0106017 [hep-ph]`.

[14] **ALICE** Collaboration, B. Abelev *et al.*, "Centrality, rapidity and transverse momentum dependence of J/Ψ suppression in Pb-Pb collisions at $\sqrt{s_{NN}}$=2.76 TeV," *Phys. Lett.* **B743** (2014) 314–327, `arXiv:1311.0214 [nucl-ex]`.

[15] **ALICE** Collaboration, J. Adam *et al.*, "Differential studies of inclusive J/ψ and ψ(2S) production at forward rapidity in Pb-Pb collisions at $\sqrt{s_{\mathrm{NN}}} = 2.76$ TeV," *JHEP* **05** (2016) 179, `arXiv:1506.08804 [nucl-ex]`.

[16] **ALICE** Collaboration, J. Adam *et al.*, "Direct photon production in Pb-Pb collisions at $\sqrt{s_{\mathrm{NN}}} = 2.76$ TeV," *Phys. Lett.* **B754** (2016) 235–248, `arXiv:1509.07324 [nucl-ex]`.

[17] P. Braun-Munzinger and J. Stachel, "(Non)thermal aspects of charmonium production and a new look at J/ψ suppression," *Phys. Lett.* **B490** (2000) 196–202.

[18] R. L. Thews, M. Schroedter, and J. Rafelski, "Enhanced J/ψ production in deconfined quark matter," *Phys. Rev.* **C63** (2001) 054905, `arXiv:hep-ph/0007323 [hep-ph]`.

[19] T. Bhattacharya *et al.*, "QCD Phase Transition with Chiral Quarks and Physical Quark Masses," *Phys. Rev. Lett.* **113** no. 8, (2014) 082001, `arXiv:1402.5175 [hep-lat]`.

[20] **ALICE** Collaboration, K. Aamodt *et al.*, "The ALICE experiment at the CERN LHC," *JINST* **3** (2008) S08002.

[21] **ALICE** Collaboration, B. Abelev *et al.*, "Performance of the ALICE Experiment at the CERN LHC," *Int. J. Mod. Phys.* **A29** (2014) 1430044, `arXiv:1402.4476 [nucl-ex]`.

[22] **ALICE** Collaboration, K. Aamodt *et al.*, "Rapidity and transverse momentum dependence of inclusive J/ψ production in pp collisions at $\sqrt{s} = 7$ TeV," *Phys. Lett.* **B704** (2011) 442–455, `arXiv:1105.0380 [hep-ex]`.

[23] **ALICE** Collaboration, K. Aamodt *et al.*, "Alignment of the ALICE Inner Tracking System with cosmic-ray tracks," *JINST* **5** (2010) P03003, `arXiv:1001.0502 [physics.ins-det]`.

[24] **ALICE** Collaboration, E. Abbas *et al.*, "Performance of the ALICE VZERO system," *JINST* **8** (2013) P10016, `arXiv:1306.3130 [nucl-ex]`.

[25] M. Bondila *et al.*, "ALICE T0 detector," *IEEE Trans. Nucl. Sci.* **52** (2005) 1705–1711.

[26] **ALICE** Collaboration, B. Abelev *et al.*, "Measurement of the Cross Section for Electromagnetic Dissociation with Neutron Emission in Pb-Pb Collisions at $\sqrt{s_{NN}} = 2.76$ TeV," *Phys. Rev. Lett.* **109** (2012) 252302, `arXiv:1203.2436 [nucl-ex]`.

[27] **ALICE** Collaboration, B. Abelev *et al.*, "Centrality determination of Pb-Pb collisions at $\sqrt{s_{NN}} =$ 2.76 TeV with ALICE," *Phys. Rev.* **C88** no. 4, (2013) 044909, `arXiv:1301.4361 [nucl-ex]`.

[28] **ALICE** Collaboration, J. Adam *et al.*, "Centrality dependence of the charged-particle multiplicity density at midrapidity in Pb-Pb collisions at $\sqrt{s_{\mathrm{NN}}} = 5.02$ TeV," *Phys. Rev. Lett.* **116** no. 22, (2016) 222302, `arXiv:1512.06104 [nucl-ex]`.

[29] ALICE Collaboration, "Quarkonium signal extraction in ALICE," *ALICE-PUBLIC-2015-006* (2015) .

[30] **ALICE** Collaboration, B. Abelev *et al.*, "Suppression of ψ(2S) production in p-Pb collisions at $\sqrt{s_{\mathrm{NN}}} = 5.02$ TeV," *JHEP* **12** (2014) 073, `arXiv:1405.3796 [nucl-ex]`.

[31] **GEANT4** Collaboration, S. Agostinelli *et al.*, "GEANT4: A Simulation toolkit," *Nucl. Instrum. Meth.* **A506** (2003) 250–303.

[32] R. Brun, F. Carminati, and S. Giani, "GEANT Detector Description and Simulation Tool," *CERN Program Library Long Writeup* **CERN-W5013** (1994) .

[33] **Particle Data Group** Collaboration, K. A. Olive *et al.*, "Review of Particle Physics," *Chin. Phys.* **C38** (2014) 090001.

[34] **ALICE** Collaboration, B. Abelev *et al.*, "J/ψ production and nuclear effects in p-Pb collisions at $\sqrt{s_{\mathrm{NN}}} = 5.02$ TeV," *JHEP* **1402** (2014) 073, `arXiv:1308.6726 [nucl-ex]`.

[35] **ALICE Collaboration** Collaboration, "Centrality dependence of the charged-particle multiplicity density at midrapidity in Pb-Pb collisions at $\sqrt{s_{\mathrm{NN}}} = 5.02$ TeV,". `https://cds.cern.ch/record/2118084`.

[36] **ALICE** Collaboration, J. Adam *et al.*, "Centrality dependence of particle production in p-Pb collisions at $\sqrt{s_{\mathrm{NN}}} = 5.02$ TeV," *Phys. Rev.* **C91** no. 6, (2015) 064905, `arXiv:1412.6828 [nucl-ex]`.

[37] **ALICE** Collaboration, B. Abelev *et al.*, "J/ψ polarization in pp collisions at $\sqrt{s} = 7$ TeV," *Phys. Rev. Lett.* **108** (2012) 082001, `arXiv:1111.1630 [hep-ex]`.

[38] **LHCb** Collaboration, R. Aaij *et al.*, "Measurement of J/ψ production in pp collisions at $\sqrt{s} = 7$ TeV," *Eur. Phys. J.* **C71** (2011) 1645, `arXiv:1103.0423 [hep-ex]`.

[39] **ALICE** Collaboration, "ALICE luminosity determination for pp collisions at $\sqrt{s} = 13$ TeV," *ALICE-PUBLIC-2016-002* (Jun, 2016) . `http://cds.cern.ch/record/2160174`.

[40] ALICE and LHCb Collaborations, "Reference pp cross-sections for J/ψ studies in proton-lead collisions at $\sqrt{s_{NN}} = 5.02$ TeV and comparisons between ALICE and LHCb results, LHCb-CONF-2013-013, ALICE-PUBLIC-2013-002,".

[41] **LHCb** Collaboration, R. Aaij *et al.*, "Measurement of J/ψ production in pp collisions at $\sqrt{s} = 2.76$ TeV," *JHEP* **02** (2013) 041, `arXiv:1212.1045 [hep-ex]`.

[42] **ALICE** Collaboration, J. Adam *et al.*, "Rapidity and transverse-momentum dependence of the inclusive J/ψ nuclear modification factor in p-Pb collisions at $\sqrt{s_{N\,N}} = 5.02$ TeV," *JHEP* **06** (2015) 055, `arXiv:1503.07179 [nucl-ex]`.

[43] **ALICE** Collaboration, B. Abelev *et al.*, "Inclusive J/ψ production in pp collisions at $\sqrt{s} = 2.76$ TeV," *Phys. Lett.* **B718** (2012) 295–306, `arXiv:1203.3641 [hep-ex]`.

[44] **ALICE** Collaboration, B. Abelev *et al.*, "Measurement of quarkonium production at forward rapidity in pp collisions at $\sqrt{s} = 7$ TeV," *Eur. Phys. J.* **C74** (2014) 2974, `arXiv:1403.3648 [nucl-ex]`.

[45] **ALICE** Collaboration, J. Adam *et al.*, "Centrality dependence of inclusive J/ψ production in p-Pb collisions at $\sqrt{s_{NN}} = 5.02$ TeV," *JHEP* **11** (2015) 127, `arXiv:1506.08808 [nucl-ex]`.

[46] **ALICE** Collaboration, J. Adam *et al.*, "Measurement of an excess in the yield of J/ψ at very low p_T in Pb-Pb collisions at $\sqrt{s_{NN}} = 2.76$ TeV," `arXiv:1509.08802 [nucl-ex]`.

[47] A. Andronic, P. Braun-Munzinger, K. Redlich, and J. Stachel, "The statistical model in Pb-Pb collisions at the LHC," *Nucl. Phys.* **A904-905** (2013) 535c–538c, `arXiv:1210.7724 [nucl-th]`.

[48] E. G. Ferreiro, "Charmonium dissociation and recombination at LHC: Revisiting comovers," *Phys. Lett.* **B731** (2014) 57–63, `arXiv:1210.3209 [hep-ph]`.

[49] E. G. Ferreiro, "Excited charmonium suppression in proton-nucleus collisions as a consequence of comovers," *Phys. Lett.* **B749** (2015) 98–103, `arXiv:1411.0549 [hep-ph]`.

[50] X. Zhao and R. Rapp, "Medium Modifications and Production of Charmonia at LHC," *Nucl. Phys.* **A859** (2011) 114–125, `arXiv:1102.2194 [hep-ph]`.

[51] X. Du and R. Rapp, "Sequential Regeneration of Charmonia in Heavy-Ion Collisions," *Nucl. Phys.* **A943** (2015) 147–158, `arXiv:1504.00670 [hep-ph]`.

[52] K. Zhou, N. Xu, Z. Xu, and P. Zhuang, "Medium effects on charmonium production at ultrarelativistic energies available at the CERN Large Hadron Collider," *Phys. Rev.* **C89** no. 5, (2014) 054911, `arXiv:1401.5845 [nucl-th]`.

[53] **LHCb** Collaboration, R. Aaij *et al.*, "Prompt charm production in pp collisions at $\sqrt{s} = 7$ TeV," *Nucl. Phys.* **B871** (2013) 1–20, `arXiv:1302.2864 [hep-ex]`.

[54] M. Cacciari, S. Frixione, N. Houdeau, M. L. Mangano, P. Nason, and G. Ridolfi, "Theoretical predictions for charm and bottom production at the LHC," *JHEP* **10** (2012) 137, `arXiv:1205.6344 [hep-ph]`.

[55] K. J. Eskola, H. Paukkunen, and C. A. Salgado, "EPS09: A New Generation of NLO and LO Nuclear Parton Distribution Functions," *JHEP* **0904** (2009) 065, `arXiv:0902.4154 [hep-ph]`.

[56] V. N. Gribov, "Glauber corrections and the interaction between high-energy hadrons and nuclei," *Sov. Phys. JETP* **29** (1969) 483–487. [Zh. Eksp. Teor. Fiz.56,892(1969)].

[57] K. J. Eskola, V. J. Kolhinen, and C. A. Salgado, "The Scale dependent nuclear effects in parton distributions for practical applications," *Eur. Phys. J.* **C9** (1999) 61–68, `arXiv:hep-ph/9807297 [hep-ph]`.

[58] D. de Florian and R. Sassot, "Nuclear parton distributions at next-to-leading order," *Phys. Rev.* **D69** (2004) 074028, `arXiv:hep-ph/0311227 [hep-ph]`.

A The ALICE Collaboration

J. Adam[40], D. Adamová[86], M.M. Aggarwal[90], G. Aglieri Rinella[36], M. Agnello[32,112], N. Agrawal[49], Z. Ahammed[135], S. Ahmad[19], S.U. Ahn[70], S. Aiola[139], A. Akindinov[60], S.N. Alam[135], D.S.D. Albuquerque[123], D. Aleksandrov[82], B. Alessandro[112], D. Alexandre[103], R. Alfaro Molina[66], A. Alici[12,106], A. Alkin[3], J. Alme[18,38], T. Alt[43], S. Altinpinar[18], I. Altsybeev[134], C. Alves Garcia Prado[122], M. An[7], C. Andrei[80], H.A. Andrews[103], A. Andronic[99], V. Anguelov[96], C. Anson[89], T. Antičić[100], F. Antinori[109], P. Antonioli[106], L. Aphecetche[115], H. Appelshäuser[55], S. Arcelli[27], R. Arnaldi[112], O.W. Arnold[37,95], I.C. Arsene[22], M. Arslandok[55], B. Audurier[115], A. Augustinus[36], R. Averbeck[99], M.D. Azmi[19], A. Badalà[108], Y.W. Baek[69], S. Bagnasco[112], R. Bailhache[55], R. Bala[93], S. Balasubramanian[139], A. Baldisseri[15], R.C. Baral[63], A.M. Barbano[26], R. Barbera[28], F. Barile[33], G.G. Barnaföldi[138], L.S. Barnby[103,36], V. Barret[72], P. Bartalini[7], K. Barth[36], J. Bartke[119,i], E. Bartsch[55], M. Basile[27], N. Bastid[72], S. Basu[135], B. Bathen[56], G. Batigne[115], A. Batista Camejo[72], B. Batyunya[68], P.C. Batzing[22], I.G. Bearden[83], H. Beck[55,96], C. Bedda[112], N.K. Behera[52], I. Belikov[57], F. Bellini[27], H. Bello Martinez[2], R. Bellwied[124], R. Belmont[137], E. Belmont-Moreno[66], L.G.E. Beltran[121], V. Belyaev[77], G. Bencedi[138], S. Beole[26], I. Berceanu[80], A. Bercuci[80], Y. Berdnikov[88], D. Berenyi[138], R.A. Bertens[59], D. Berzano[36], L. Betev[36], A. Bhasin[93], I.R. Bhat[93], A.K. Bhati[90], B. Bhattacharjee[45], J. Bhom[119], L. Bianchi[124], N. Bianchi[74], C. Bianchin[137], J. Bielčík[40], J. Bielčíková[86], A. Bilandzic[83,37,95], G. Biro[138], R. Biswas[4], S. Biswas[4,81], S. Bjelogrlic[59], J.T. Blair[120], D. Blau[82], C. Blume[55], F. Bock[76,96], A. Bogdanov[77], H. Bøggild[83], L. Boldizsár[138], M. Bombara[41], M. Bonora[36], J. Book[55], H. Borel[15], A. Borissov[98], M. Borri[85,126], F. Bossú[67], E. Botta[26], C. Bourjau[83], P. Braun-Munzinger[99], M. Bregant[122], T. Breitner[54], T.A. Broker[55], T.A. Browning[97], M. Broz[40], E.J. Brucken[47], E. Bruna[112], G.E. Bruno[33], D. Budnikov[101], H. Buesching[55], S. Bufalino[26,32], P. Buncic[36], O. Busch[130], Z. Buthelezi[67], J.B. Butt[16], J.T. Buxton[20], J. Cabala[117], D. Caffarri[36], X. Cai[7], H. Caines[139], L. Calero Diaz[74], A. Caliva[59], E. Calvo Villar[104], P. Camerini[25], F. Carena[36], W. Carena[36], F. Carnesecchi[27], J. Castillo Castellanos[15], A.J. Castro[127], E.A.R. Casula[24], C. Ceballos Sanchez[9], J. Cepila[40], P. Cerello[112], J. Cerkala[117], B. Chang[125], S. Chapeland[36], M. Chartier[126], J.L. Charvet[15], S. Chattopadhyay[135], S. Chattopadhyay[102], A. Chauvin[95,37], V. Chelnokov[3], M. Cherney[89], C. Cheshkov[132], B. Cheynis[132], V. Chibante Barroso[36], D.D. Chinellato[123], S. Cho[52], P. Chochula[36], K. Choi[98], M. Chojnacki[83], S. Choudhury[135], P. Christakoglou[84], C.H. Christensen[83], P. Christiansen[34], T. Chujo[130], S.U. Chung[98], C. Cicalo[107], L. Cifarelli[12,27], F. Cindolo[106], J. Cleymans[92], F. Colamaria[33], D. Colella[61,36], A. Collu[76], M. Colocci[27], G. Conesa Balbastre[73], Z. Conesa del Valle[53], M.E. Connors[ii,139], J.G. Contreras[40], T.M. Cormier[87], Y. Corrales Morales[26,112], I. Cortés Maldonado[2], P. Cortese[31], M.R. Cosentino[122], F. Costa[36], J. Crkovska[53], P. Crochet[72], R. Cruz Albino[11], E. Cuautle[65], L. Cunqueiro[56,36], T. Dahms[37,95], A. Dainese[109], M.C. Danisch[96], A. Danu[64], D. Das[102], I. Das[102], S. Das[4], A. Dash[81], S. Dash[49], S. De[122], A. De Caro[30], G. de Cataldo[105], C. de Conti[122], J. de Cuveland[43], A. De Falco[24], D. De Gruttola[12,30], N. De Marco[112], S. De Pasquale[30], R.D. De Souza[123], A. Deisting[96,99], A. Deloff[79], C. Deplano[84], P. Dhankher[49], D. Di Bari[33], A. Di Mauro[36], P. Di Nezza[74], B. Di Ruzza[109], M.A. Diaz Corchero[10], T. Dietel[92], P. Dillenseger[55], R. Divià[36], Ø. Djuvsland[18], A. Dobrin[84,64], D. Domenicis Gimenez[122], B. Dönigus[55], O. Dordic[22], T. Drozhzhova[55], A.K. Dubey[135], A. Dubla[59], L. Ducroux[132], P. Dupieux[72], R.J. Ehlers[139], D. Elia[105], E. Endress[104], H. Engel[54], E. Epple[139], B. Erazmus[115], I. Erdemir[55], F. Erhardt[131], B. Espagnon[53], M. Estienne[115], S. Esumi[130], G. Eulisse[36], J. Eum[98], D. Evans[103], S. Evdokimov[113], G. Eyyubova[40], L. Fabbietti[95,37], D. Fabris[109], J. Faivre[73], A. Fantoni[74], M. Fasel[76], L. Feldkamp[56], A. Feliciello[112], G. Feofilov[134], J. Ferencei[86], A. Fernández Téllez[2], E.G. Ferreiro[17], A. Ferretti[26], A. Festanti[29], V.J.G. Feuillard[15,72], J. Figiel[119], M.A.S. Figueredo[122], S. Filchagin[101], D. Finogeev[58], F.M. Fionda[24], E.M. Fiore[33], M. Floris[36], S. Foertsch[67], P. Foka[99], S. Fokin[82], E. Fragiacomo[111], A. Francescon[36], A. Francisco[115], U. Frankenfeld[99], G.G. Fronze[26], U. Fuchs[36], C. Furget[73], A. Furs[58], M. Fusco Girard[30], J.J. Gaardhøje[83], M. Gagliardi[26], A.M. Gago[104], K. Gajdosova[83], M. Gallio[26], C.D. Galvan[121], D.R. Gangadharan[76], P. Ganoti[91], C. Gao[7], C. Garabatos[99], E. Garcia-Solis[13], K. Garg[28], C. Gargiulo[36], P. Gasik[95,37], E.F. Gauger[120], M. Germain[115], M. Gheata[36,64], P. Ghosh[135], S.K. Ghosh[4], P. Gianotti[74], P. Giubellino[112,36], P. Giubilato[29], E. Gladysz-Dziadus[119], P. Glässel[96], D.M. Gómez Coral[66], A. Gomez Ramirez[54], A.S. Gonzalez[36], V. Gonzalez[10], P. González-Zamora[10], S. Gorbunov[43], L. Görlich[119], S. Gotovac[118], V. Grabski[66], O.A. Grachov[139], L.K. Graczykowski[136], K.L. Graham[103], A. Grelli[59], A. Grigoras[36], C. Grigoras[36], V. Grigoriev[77], A. Grigoryan[1], S. Grigoryan[68], B. Grinyov[3], N. Grion[111], J.M. Gronefeld[99], J.F. Grosse-Oetringhaus[36], R. Grosso[99], L. Gruber[114], F. Guber[58], R. Guernane[73], B. Guerzoni[27], K. Gulbrandsen[83], T. Gunji[129], A. Gupta[93], R. Gupta[93], I.B. Guzman[2], R. Haake[56,36], C. Hadjidakis[53], M. Haiduc[64], H. Hamagaki[129], G. Hamar[138], J.C. Hamon[57], J.W. Harris[139], A. Harton[13], D. Hatzifotiadou[106], S. Hayashi[129], S.T. Heckel[55], E. Hellbär[55], H. Helstrup[38], A. Herghelegiu[80],

G. Herrera Corral[11], F. Herrmann[56], B.A. Hess[35], K.F. Hetland[38], H. Hillemanns[36], B. Hippolyte[57], D. Horak[40], R. Hosokawa[130], P. Hristov[36], C. Hughes[127], T.J. Humanic[20], N. Hussain[45], T. Hussain[19], D. Hutter[43], D.S. Hwang[21], R. Ilkaev[101], M. Inaba[130], E. Incani[24], M. Ippolitov[77,82], M. Irfan[19], V. Isakov[58], M. Ivanov[99,36], V. Ivanov[88], V. Izucheev[113], B. Jacak[76], N. Jacazio[27], P.M. Jacobs[76], M.B. Jadhav[49], S. Jadlovska[117], J. Jadlovsky[117,61], C. Jahnke[122,37], M.J. Jakubowska[136], M.A. Janik[136], P.H.S.Y. Jayarathna[124], C. Jena[29], S. Jena[124], R.T. Jimenez Bustamante[99], P.G. Jones[103], H. Jung[44], A. Jusko[103], P. Kalinak[61], A. Kalweit[36], J.H. Kang[140], V. Kaplin[77], S. Kar[135], A. Karasu Uysal[71], O. Karavichev[58], T. Karavicheva[58], L. Karayan[99,96], E. Karpechev[58], U. Kebschull[54], R. Keidel[141], D.L.D. Keijdener[59], M. Keil[36], M. Mohisin Khan[iii,19], P. Khan[102], S.A. Khan[135], A. Khanzadeev[88], Y. Kharlov[113], A. Khatun[19], B. Kileng[38], D.W. Kim[44], D.J. Kim[125], D. Kim[140], H. Kim[140], J.S. Kim[44], J. Kim[96], M. Kim[52], M. Kim[140], S. Kim[21], T. Kim[140], S. Kirsch[43], I. Kisel[43], S. Kiselev[60], A. Kisiel[136], G. Kiss[138], J.L. Klay[6], C. Klein[55], J. Klein[36], C. Klein-Bösing[56], S. Klewin[96], A. Kluge[36], M.L. Knichel[96], A.G. Knospe[120,124], C. Kobdaj[116], M. Kofarago[36], T. Kollegger[99], A. Kolojvari[134], V. Kondratiev[134], N. Kondratyeva[77], E. Kondratyuk[113], A. Konevskikh[58], M. Kopcik[117], M. Kour[93], C. Kouzinopoulos[36], O. Kovalenko[79], V. Kovalenko[134], M. Kowalski[119], G. Koyithatta Meethaleveedu[49], I. Králik[61], A. Kravčáková[41], M. Krivda[61,103], F. Krizek[86], E. Kryshen[88,36], M. Krzewicki[43], A.M. Kubera[20], V. Kučera[86], C. Kuhn[57], P.G. Kuijer[84], A. Kumar[93], J. Kumar[49], L. Kumar[90], S. Kumar[49], P. Kurashvili[79], A. Kurepin[58], A.B. Kurepin[58], A. Kuryakin[101], M.J. Kweon[52], Y. Kwon[140], S.L. La Pointe[112,43], P. La Rocca[28], P. Ladron de Guevara[11], C. Lagana Fernandes[122], I. Lakomov[36], R. Langoy[42], K. Lapidus[37,139], C. Lara[54], A. Lardeux[15], A. Lattuca[26], E. Laudi[36], R. Lea[25], L. Leardini[96], S. Lee[140], F. Lehas[84], S. Lehner[114], R.C. Lemmon[85], V. Lenti[105], E. Leogrande[59], I. León Monzón[121], H. León Vargas[66], M. Leoncino[26], P. Lévai[138], S. Li[7,72], X. Li[14], J. Lien[42], R. Lietava[103], S. Lindal[22], V. Lindenstruth[43], C. Lippmann[99], M.A. Lisa[20], H.M. Ljunggren[34], D.F. Lodato[59], P.I. Loenne[18], V. Loginov[77], C. Loizides[76], X. Lopez[72], E. López Torres[9], A. Lowe[138], P. Luettig[55], M. Lunardon[29], G. Luparello[25], M. Lupi[36], T.H. Lutz[139], A. Maevskaya[58], M. Mager[36], S. Mahajan[93], S.M. Mahmood[22], A. Maire[57], R.D. Majka[139], M. Malaev[88], I. Maldonado Cervantes[65], L. Malinina[iv,68], D. Mal'Kevich[60], P. Malzacher[99], A. Mamonov[101], V. Manko[82], F. Manso[72], V. Manzari[36,105], Y. Mao[7], M. Marchisone[67,128,26], J. Mareš[62], G.V. Margagliotti[25], A. Margotti[106], J. Margutti[59], A. Marín[99], C. Markert[120], M. Marquard[55], N.A. Martin[99], P. Martinengo[36], M.I. Martínez[2], G. Martínez García[115], M. Martinez Pedreira[36], A. Mas[122], S. Masciocchi[99], M. Masera[26], A. Masoni[107], A. Mastroserio[33], A. Matyja[119], C. Mayer[119], J. Mazer[127], M. Mazzilli[33], M.A. Mazzoni[110], F. Meddi[23], Y. Melikyan[77], A. Menchaca-Rocha[66], E. Meninno[30], J. Mercado Pérez[96], M. Meres[39], S. Mhlanga[92], Y. Miake[130], M.M. Mieskolainen[47], K. Mikhaylov[60,68], L. Milano[76,36], J. Milosevic[22], A. Mischke[59], A.N. Mishra[50], T. Mishra[63], D. Miśkowiec[99], J. Mitra[135], C.M. Mitu[64], N. Mohammadi[59], B. Mohanty[81], L. Molnar[57], L. Montaño Zetina[11], E. Montes[10], D.A. Moreira De Godoy[56], L.A.P. Moreno[2], S. Moretto[29], A. Morreale[115], A. Morsch[36], V. Muccifora[74], E. Mudnic[118], D. Mühlheim[56], S. Muhuri[135], M. Mukherjee[135], J.D. Mulligan[139], M.G. Munhoz[122], K. Münning[46], R.H. Munzer[37,55,95], H. Murakami[129], S. Murray[67], L. Musa[36], J. Musinsky[61], B. Naik[49], R. Nair[79], B.K. Nandi[49], R. Nania[106], E. Nappi[105], M.U. Naru[16], H. Natal da Luz[122], C. Nattrass[127], S.R. Navarro[2], K. Nayak[81], R. Nayak[49], T.K. Nayak[135], S. Nazarenko[101], A. Nedosekin[60], R.A. Negrao De Oliveira[36], L. Nellen[65], F. Ng[124], M. Nicassio[99], M. Niculescu[64], J. Niedziela[36], B.S. Nielsen[83], S. Nikolaev[82], S. Nikulin[82], V. Nikulin[88], F. Noferini[106,12], P. Nomokonov[68], G. Nooren[59], J.C.C. Noris[2], J. Norman[126], A. Nyanin[82], J. Nystrand[18], H. Oeschler[96], S. Oh[139], S.K. Oh[69], A. Ohlson[36], A. Okatan[71], T. Okubo[48], J. Oleniacz[136], A.C. Oliveira Da Silva[122], M.H. Oliver[139], J. Onderwaater[99], C. Oppedisano[112], R. Orava[47], M. Oravec[117], A. Ortiz Velasquez[65], A. Oskarsson[34], J. Otwinowski[119], K. Oyama[96,78], M. Ozdemir[55], Y. Pachmayer[96], D. Pagano[133], P. Pagano[30], G. Paić[65], S.K. Pal[135], P. Palni[7], J. Pan[137], A.K. Pandey[49], V. Papikyan[1], G.S. Pappalardo[108], P. Pareek[50], J. Park[52], W.J. Park[99], S. Parmar[90], A. Passfeld[56], V. Paticchio[105], R.N. Patra[135], B. Paul[112], H. Pei[7], T. Peitzmann[59], X. Peng[7], H. Pereira Da Costa[15], D. Peresunko[77,82], E. Perez Lezama[55], V. Peskov[55], Y. Pestov[5], V. Petráček[40], V. Petrov[113], M. Petrovici[80], C. Petta[28], S. Piano[111], M. Pikna[39], P. Pillot[115], L.O.D.L. Pimentel[83], O. Pinazza[106,36], L. Pinsky[124], D.B. Piyarathna[124], M. Płoskoń[76], M. Planinic[131], J. Pluta[136], S. Pochybova[138], P.L.M. Podesta-Lerma[121], M.G. Poghosyan[87], B. Polichtchouk[113], N. Poljak[131], W. Poonsawat[116], A. Pop[80], H. Poppenborg[56], S. Porteboeuf-Houssais[72], J. Porter[76], J. Pospisil[86], S.K. Prasad[4], R. Preghenella[106,36], F. Prino[112], C.A. Pruneau[137], I. Pshenichnov[58], M. Puccio[26], G. Puddu[24], P. Pujahari[137], V. Punin[101], J. Putschke[137], H. Qvigstad[22], A. Rachevski[111], S. Raha[4], S. Rajput[93], J. Rak[125], A. Rakotozafindrabe[15], L. Ramello[31], F. Rami[57], R. Raniwala[94], S. Raniwala[94], S.S. Räsänen[47], B.T. Rascanu[55], D. Rathee[90], V. Ratza[46], I. Ravasenga[26], K.F. Read[127,87], K. Redlich[79], R.J. Reed[137], A. Rehman[18], P. Reichelt[55], F. Reidt[36,96], X. Ren[7], R. Renfordt[55], A.R. Reolon[74], A. Reshetin[58],

K. Reygers[96], V. Riabov[88], R.A. Ricci[75], T. Richert[34], M. Richter[22], P. Riedler[36], W. Riegler[36], F. Riggi[28], C. Ristea[64], M. Rodríguez Cahuantzi[2], A. Rodriguez Manso[84], K. Røed[22], E. Rogochaya[68], D. Rohr[43], D. Röhrich[18], F. Ronchetti[36,74], L. Ronflette[115], P. Rosnet[72], A. Rossi[29], F. Roukoutakis[91], A. Roy[50], C. Roy[57], P. Roy[102], A.J. Rubio Montero[10], R. Rui[25], R. Russo[26], E. Ryabinkin[82], Y. Ryabov[88], A. Rybicki[119], S. Saarinen[47], S. Sadhu[135], S. Sadovsky[113], K. Šafařík[36], B. Sahlmuller[55], P. Sahoo[50], R. Sahoo[50], S. Sahoo[63], P.K. Sahu[63], J. Saini[135], S. Sakai[74], M.A. Saleh[137], J. Salzwedel[20], S. Sambyal[93], V. Samsonov[88,77], L. Šándor[61], A. Sandoval[66], M. Sano[130], D. Sarkar[135], N. Sarkar[135], P. Sarma[45], E. Scapparone[106], F. Scarlassara[29], C. Schiaua[80], R. Schicker[96], C. Schmidt[99], H.R. Schmidt[35], M. Schmidt[35], S. Schuchmann[55,96], J. Schukraft[36], Y. Schutz[36,115], K. Schwarz[99], K. Schweda[99], G. Scioli[27], E. Scomparin[112], R. Scott[127], M. Šefčík[41], J.E. Seger[89], Y. Sekiguchi[129], D. Sekihata[48], I. Selyuzhenkov[99], K. Senosi[67], S. Senyukov[3,36], E. Serradilla[10,66], A. Sevcenco[64], A. Shabanov[58], A. Shabetai[115], O. Shadura[3], R. Shahoyan[36], A. Shangaraev[113], A. Sharma[93], M. Sharma[93], M. Sharma[93], N. Sharma[127], A.I. Sheikh[135], K. Shigaki[48], Q. Shou[7], K. Shtejer[9,26], Y. Sibiriak[82], S. Siddhanta[107], K.M. Sielewicz[36], T. Siemiarczuk[79], D. Silvermyr[34], C. Silvestre[73], G. Simatovic[131], G. Simonetti[36], R. Singaraju[135], R. Singh[81], V. Singhal[135], T. Sinha[102], B. Sitar[39], M. Sitta[31], T.B. Skaali[22], M. Slupecki[125], N. Smirnov[139], R.J.M. Snellings[59], T.W. Snellman[125], J. Song[98], M. Song[140], Z. Song[7], F. Soramel[29], S. Sorensen[127], F. Sozzi[99], E. Spiriti[74], I. Sputowska[119], M. Spyropoulou-Stassinaki[91], J. Stachel[96], I. Stan[64], P. Stankus[87], E. Stenlund[34], G. Steyn[67], J.H. Stiller[96], D. Stocco[115], P. Strmen[39], A.A.P. Suaide[122], T. Sugitate[48], C. Suire[53], M. Suleymanov[16], M. Suljic[25,i], R. Sultanov[60], M. Šumbera[86], S. Sumowidagdo[51], S. Swain[63], A. Szabo[39], I. Szarka[39], A. Szczepankiewicz[136], M. Szymanski[136], U. Tabassam[16], J. Takahashi[123], G.J. Tambave[18], N. Tanaka[130], M. Tarhini[53], M. Tariq[19], M.G. Tarzila[80], A. Tauro[36], G. Tejeda Muñoz[2], A. Telesca[36], K. Terasaki[129], C. Terrevoli[29], B. Teyssier[132], J. Thäder[76], D. Thakur[50], D. Thomas[120], R. Tieulent[132], A. Tikhonov[58], A.R. Timmins[124], A. Toia[55], S. Trogolo[26], G. Trombetta[33], V. Trubnikov[3], W.H. Trzaska[125], T. Tsuji[129], A. Tumkin[101], R. Turrisi[109], T.S. Tveter[22], K. Ullaland[18], A. Uras[132], G.L. Usai[24], A. Utrobicic[131], M. Vala[61], L. Valencia Palomo[72], J. Van Der Maarel[59], J.W. Van Hoorne[36,114], M. van Leeuwen[59], T. Vanat[86], P. Vande Vyvre[36], D. Varga[138], A. Vargas[2], M. Vargyas[125], R. Varma[49], M. Vasileiou[91], A. Vasiliev[82], A. Vauthier[73], O. Vázquez Doce[95,37], V. Vechernin[134], A.M. Veen[59], A. Velure[18], E. Vercellin[26], S. Vergara Limón[2], R. Vernet[8], L. Vickovic[118], J. Viinikainen[125], Z. Vilakazi[128], O. Villalobos Baillie[103], A. Villatoro Tello[2], A. Vinogradov[82], L. Vinogradov[134], T. Virgili[30], V. Vislavicius[34], Y.P. Viyogi[135], A. Vodopyanov[68], M.A. Völkl[96], K. Voloshin[60], S.A. Voloshin[137], G. Volpe[33,138], B. von Haller[36], I. Vorobyev[95,37], D. Vranic[99,36], J. Vrláková[41], B. Vulpescu[72], B. Wagner[18], J. Wagner[99], H. Wang[59], M. Wang[7], D. Watanabe[130], Y. Watanabe[129], M. Weber[36,114], S.G. Weber[99], D.F. Weiser[96], J.P. Wessels[56], U. Westerhoff[56], A.M. Whitehead[92], J. Wiechula[35], J. Wikne[22], G. Wilk[79], J. Wilkinson[96], G.A. Willems[56], M.C.S. Williams[106], B. Windelband[96], M. Winn[96], S. Yalcin[71], P. Yang[7], S. Yano[48], Z. Yin[7], H. Yokoyama[130], I.-K. Yoo[98], J.H. Yoon[52], V. Yurchenko[3], V. Zaccolo[83], A. Zaman[16], C. Zampolli[106,36], H.J.C. Zanoli[122], S. Zaporozhets[68], N. Zardoshti[103], A. Zarochentsev[134], P. Závada[62], N. Zaviyalov[101], H. Zbroszczyk[136], I.S. Zgura[64], M. Zhalov[88], H. Zhang[18,7], X. Zhang[7,76], Y. Zhang[7], C. Zhang[59], Z. Zhang[7], C. Zhao[22], N. Zhigareva[60], D. Zhou[7], Y. Zhou[83], Z. Zhou[18], H. Zhu[18,7], J. Zhu[7,115], A. Zichichi[12,27], A. Zimmermann[96], M.B. Zimmermann[56,36], G. Zinovjev[3], M. Zyzak[43]

Affiliation notes

[i] Deceased

[ii] Also at: Georgia State University, Atlanta, Georgia, United States

[iii] Also at: Also at Department of Applied Physics, Aligarh Muslim University, Aligarh, India

[iv] Also at: M.V. Lomonosov Moscow State University, D.V. Skobeltsyn Institute of Nuclear, Physics, Moscow, Russia

Collaboration Institutes

[1] A.I. Alikhanyan National Science Laboratory (Yerevan Physics Institute) Foundation, Yerevan, Armenia

[2] Benemérita Universidad Autónoma de Puebla, Puebla, Mexico

[3] Bogolyubov Institute for Theoretical Physics, Kiev, Ukraine

[4] Bose Institute, Department of Physics and Centre for Astroparticle Physics and Space Science (CAPSS), Kolkata, India

[5] Budker Institute for Nuclear Physics, Novosibirsk, Russia

[6] California Polytechnic State University, San Luis Obispo, California, United States

[7] Central China Normal University, Wuhan, China

[8] Centre de Calcul de l'IN2P3, Villeurbanne, France

[9] Centro de Aplicaciones Tecnológicas y Desarrollo Nuclear (CEADEN), Havana, Cuba

[10] Centro de Investigaciones Energéticas Medioambientales y Tecnológicas (CIEMAT), Madrid, Spain

[11] Centro de Investigación y de Estudios Avanzados (CINVESTAV), Mexico City and Mérida, Mexico

[12] Centro Fermi - Museo Storico della Fisica e Centro Studi e Ricerche "Enrico Fermi", Rome, Italy

[13] Chicago State University, Chicago, Illinois, USA

[14] China Institute of Atomic Energy, Beijing, China

[15] Commissariat à l'Energie Atomique, IRFU, Saclay, France

[16] COMSATS Institute of Information Technology (CIIT), Islamabad, Pakistan

[17] Departamento de Física de Partículas and IGFAE, Universidad de Santiago de Compostela, Santiago de Compostela, Spain

[18] Department of Physics and Technology, University of Bergen, Bergen, Norway

[19] Department of Physics, Aligarh Muslim University, Aligarh, India

[20] Department of Physics, Ohio State University, Columbus, Ohio, United States

[21] Department of Physics, Sejong University, Seoul, South Korea

[22] Department of Physics, University of Oslo, Oslo, Norway

[23] Dipartimento di Fisica dell'Università 'La Sapienza' and Sezione INFN Rome, Italy

[24] Dipartimento di Fisica dell'Università and Sezione INFN, Cagliari, Italy

[25] Dipartimento di Fisica dell'Università and Sezione INFN, Trieste, Italy

[26] Dipartimento di Fisica dell'Università and Sezione INFN, Turin, Italy

[27] Dipartimento di Fisica e Astronomia dell'Università and Sezione INFN, Bologna, Italy

[28] Dipartimento di Fisica e Astronomia dell'Università and Sezione INFN, Catania, Italy

[29] Dipartimento di Fisica e Astronomia dell'Università and Sezione INFN, Padova, Italy

[30] Dipartimento di Fisica 'E.R. Caianiello' dell'Università and Gruppo Collegato INFN, Salerno, Italy

[31] Dipartimento di Scienze e Innovazione Tecnologica dell'Università del Piemonte Orientale and Gruppo Collegato INFN, Alessandria, Italy

[32] Dipartimento DISAT del Politecnico and Sezione INFN, Turin, Italy

[33] Dipartimento Interateneo di Fisica 'M. Merlin' and Sezione INFN, Bari, Italy

[34] Division of Experimental High Energy Physics, University of Lund, Lund, Sweden

[35] Eberhard Karls Universität Tübingen, Tübingen, Germany

[36] European Organization for Nuclear Research (CERN), Geneva, Switzerland

[37] Excellence Cluster Universe, Technische Universität München, Munich, Germany

[38] Faculty of Engineering, Bergen University College, Bergen, Norway

[39] Faculty of Mathematics, Physics and Informatics, Comenius University, Bratislava, Slovakia

[40] Faculty of Nuclear Sciences and Physical Engineering, Czech Technical University in Prague, Prague, Czech Republic

[41] Faculty of Science, P.J. Šafárik University, Košice, Slovakia

[42] Faculty of Technology, Buskerud and Vestfold University College, Vestfold, Norway

[43] Frankfurt Institute for Advanced Studies, Johann Wolfgang Goethe-Universität Frankfurt, Frankfurt, Germany

[44] Gangneung-Wonju National University, Gangneung, South Korea

[45] Gauhati University, Department of Physics, Guwahati, India

[46] Helmholtz-Institut für Strahlen- und Kernphysik, Rheinische Friedrich-Wilhelms-Universität Bonn, Bonn, Germany

[47] Helsinki Institute of Physics (HIP), Helsinki, Finland

[48] Hiroshima University, Hiroshima, Japan

[49] Indian Institute of Technology Bombay (IIT), Mumbai, India

[50] Indian Institute of Technology Indore, Indore (IITI), India

[51] Indonesian Institute of Sciences, Jakarta, Indonesia

[52] Inha University, Incheon, South Korea

[53] Institut de Physique Nucléaire d'Orsay (IPNO), Université Paris-Sud, CNRS-IN2P3, Orsay, France

[54] Institut für Informatik, Johann Wolfgang Goethe-Universität Frankfurt, Frankfurt, Germany

[55] Institut für Kernphysik, Johann Wolfgang Goethe-Universität Frankfurt, Frankfurt, Germany

[56] Institut für Kernphysik, Westfälische Wilhelms-Universität Münster, Münster, Germany

[57] Institut Pluridisciplinaire Hubert Curien (IPHC), Université de Strasbourg, CNRS-IN2P3, Strasbourg,

France
[58] Institute for Nuclear Research, Academy of Sciences, Moscow, Russia
[59] Institute for Subatomic Physics of Utrecht University, Utrecht, Netherlands
[60] Institute for Theoretical and Experimental Physics, Moscow, Russia
[61] Institute of Experimental Physics, Slovak Academy of Sciences, Košice, Slovakia
[62] Institute of Physics, Academy of Sciences of the Czech Republic, Prague, Czech Republic
[63] Institute of Physics, Bhubaneswar, India
[64] Institute of Space Science (ISS), Bucharest, Romania
[65] Instituto de Ciencias Nucleares, Universidad Nacional Autónoma de México, Mexico City, Mexico
[66] Instituto de Física, Universidad Nacional Autónoma de México, Mexico City, Mexico
[67] iThemba LABS, National Research Foundation, Somerset West, South Africa
[68] Joint Institute for Nuclear Research (JINR), Dubna, Russia
[69] Konkuk University, Seoul, South Korea
[70] Korea Institute of Science and Technology Information, Daejeon, South Korea
[71] KTO Karatay University, Konya, Turkey
[72] Laboratoire de Physique Corpusculaire (LPC), Clermont Université, Université Blaise Pascal, CNRS–IN2P3, Clermont-Ferrand, France
[73] Laboratoire de Physique Subatomique et de Cosmologie, Université Grenoble-Alpes, CNRS-IN2P3, Grenoble, France
[74] Laboratori Nazionali di Frascati, INFN, Frascati, Italy
[75] Laboratori Nazionali di Legnaro, INFN, Legnaro, Italy
[76] Lawrence Berkeley National Laboratory, Berkeley, California, United States
[77] Moscow Engineering Physics Institute, Moscow, Russia
[78] Nagasaki Institute of Applied Science, Nagasaki, Japan
[79] National Centre for Nuclear Studies, Warsaw, Poland
[80] National Institute for Physics and Nuclear Engineering, Bucharest, Romania
[81] National Institute of Science Education and Research, Bhubaneswar, India
[82] National Research Centre Kurchatov Institute, Moscow, Russia
[83] Niels Bohr Institute, University of Copenhagen, Copenhagen, Denmark
[84] Nikhef, Nationaal instituut voor subatomaire fysica, Amsterdam, Netherlands
[85] Nuclear Physics Group, STFC Daresbury Laboratory, Daresbury, United Kingdom
[86] Nuclear Physics Institute, Academy of Sciences of the Czech Republic, Řež u Prahy, Czech Republic
[87] Oak Ridge National Laboratory, Oak Ridge, Tennessee, United States
[88] Petersburg Nuclear Physics Institute, Gatchina, Russia
[89] Physics Department, Creighton University, Omaha, Nebraska, United States
[90] Physics Department, Panjab University, Chandigarh, India
[91] Physics Department, University of Athens, Athens, Greece
[92] Physics Department, University of Cape Town, Cape Town, South Africa
[93] Physics Department, University of Jammu, Jammu, India
[94] Physics Department, University of Rajasthan, Jaipur, India
[95] Physik Department, Technische Universität München, Munich, Germany
[96] Physikalisches Institut, Ruprecht-Karls-Universität Heidelberg, Heidelberg, Germany
[97] Purdue University, West Lafayette, Indiana, United States
[98] Pusan National University, Pusan, South Korea
[99] Research Division and ExtreMe Matter Institute EMMI, GSI Helmholtzzentrum für Schwerionenforschung, Darmstadt, Germany
[100] Rudjer Bošković Institute, Zagreb, Croatia
[101] Russian Federal Nuclear Center (VNIIEF), Sarov, Russia
[102] Saha Institute of Nuclear Physics, Kolkata, India
[103] School of Physics and Astronomy, University of Birmingham, Birmingham, United Kingdom
[104] Sección Física, Departamento de Ciencias, Pontificia Universidad Católica del Perú, Lima, Peru
[105] Sezione INFN, Bari, Italy
[106] Sezione INFN, Bologna, Italy
[107] Sezione INFN, Cagliari, Italy
[108] Sezione INFN, Catania, Italy
[109] Sezione INFN, Padova, Italy

[110] Sezione INFN, Rome, Italy

[111] Sezione INFN, Trieste, Italy

[112] Sezione INFN, Turin, Italy

[113] SSC IHEP of NRC Kurchatov institute, Protvino, Russia

[114] Stefan Meyer Institut für Subatomare Physik (SMI), Vienna, Austria

[115] SUBATECH, Ecole des Mines de Nantes, Université de Nantes, CNRS-IN2P3, Nantes, France

[116] Suranaree University of Technology, Nakhon Ratchasima, Thailand

[117] Technical University of Košice, Košice, Slovakia

[118] Technical University of Split FESB, Split, Croatia

[119] The Henryk Niewodniczanski Institute of Nuclear Physics, Polish Academy of Sciences, Cracow, Poland

[120] The University of Texas at Austin, Physics Department, Austin, Texas, USA

[121] Universidad Autónoma de Sinaloa, Culiacán, Mexico

[122] Universidade de São Paulo (USP), São Paulo, Brazil

[123] Universidade Estadual de Campinas (UNICAMP), Campinas, Brazil

[124] University of Houston, Houston, Texas, United States

[125] University of Jyväskylä, Jyväskylä, Finland

[126] University of Liverpool, Liverpool, United Kingdom

[127] University of Tennessee, Knoxville, Tennessee, United States

[128] University of the Witwatersrand, Johannesburg, South Africa

[129] University of Tokyo, Tokyo, Japan

[130] University of Tsukuba, Tsukuba, Japan

[131] University of Zagreb, Zagreb, Croatia

[132] Université de Lyon, Université Lyon 1, CNRS/IN2P3, IPN-Lyon, Villeurbanne, France

[133] Università di Brescia

[134] V. Fock Institute for Physics, St. Petersburg State University, St. Petersburg, Russia

[135] Variable Energy Cyclotron Centre, Kolkata, India

[136] Warsaw University of Technology, Warsaw, Poland

[137] Wayne State University, Detroit, Michigan, United States

[138] Wigner Research Centre for Physics, Hungarian Academy of Sciences, Budapest, Hungary

[139] Yale University, New Haven, Connecticut, United States

[140] Yonsei University, Seoul, South Korea

[141] Zentrum für Technologietransfer und Telekommunikation (ZTT), Fachhochschule Worms, Worms, Germany